Amino Acids (2008) 35: 75–82
DOI 10.1007/s00726-007-0627-8
Printed in The Netherlands

Amino Acids

Hyperactive mutants of mouse D-aspartate oxidase: mutagenesis of the active site residue serine 308

M. Katane, T. Hanai, T. Furuchi, M. Sekine, and **H. Homma**

Laboratory of Biomolecular Science, School of Pharmaceutical Sciences, Kitasato University, Tokyo, Japan

Received September 7, 2007
Accepted October 25, 2007
Published online January 31, 2008;

Summary. The role of Ser-308 of murine D-aspartate oxidase (mDASPO), particularly its side chain hydroxyl group, was investigated through the use of site-specific mutational analysis of Ser-308. Recombinant mDASPO carrying a substitution of Gly, Ala, or Tyr for Ser-308 was generated, and fused to either His (His-mDASPO), or glutathione *S*-transferase, His, and S (GHS-mDASPO) at its N-terminus. Wild-type His-mDASPO or GHS-mDASPO or their mutant derivatives were expressed in *Escherichia coli* and purified by affinity chromatography. All purified recombinant proteins had functional DASPO activity. The Gly-308 and Ala-308 mutants had significantly higher catalytic efficiency towards D-Asp and *N*-methyl-D-Asp, and a higher affinity for flavin adenine dinucleotide (FAD) compared to the wild-type enzyme. The Tyr-308 mutant had lower catalytic efficiency and binding capacity. These results suggest that the side chain hydroxyl group of a critical residue of mDASPO, Ser-308, down-regulates enzymatic activity, substrate binding, and FAD binding. This study provides information on the active site of DASPO that will considerably enhance our understanding of the biological significance of this enzyme.

Keywords: D-aspartate oxidase – Flavoprotein – Site-directed mutagenesis – D-amino acid oxidase – D-amino acid – D-aspartate

Abbreviations: DAAO, D-amino acid oxidase; DASPO, D-aspartate oxidase; FAD, flavin adenine dinucleotide; GHS, glutathione *S*-transferase, His, and S; GHS-mDASPO, N-terminally glutathione *S*-transferase-, His-, and S-tagged mouse D-aspartate oxidase; GST, glutathione *S*-transferase; His-mDASPO, N-terminally His-tagged mouse D-aspartate oxidase; $K_{d,FAD}$, dissociation constant value for binding to flavin adenine dinucleotide; mDASPO, mouse D-aspartate oxidase; NMDA, *N*-methyl-D-aspartate

Introduction

Amino acids, with the exception of Gly, have asymmetric α-carbon atoms, and can exist as one of two stereoisomers, an L- or D-isomer. While some D-amino acids are known to be essential components of cell wall peptidoglycans and antibiotic peptides in bacteria, it has long been believed that D-amino acids do not play a significant role in the physiology of higher organisms. However, recent reports have revealed that several higher organisms contain several D-amino acids, either in their free form or as components of proteins (for review, see Abe et al., 2005; Fujii, 2005; Hamase et al., 2005). Free D-Ser and D-Asp in mammals have been the subject of extensive investigation. D-Ser was found to be concentrated predominantly in the mammalian forebrain, and it has been suggested that it regulates Glu-mediated activation of *N*-methyl-D-Asp (NMDA) receptors by acting as a co-agonist (for review see Schell, 2004; Scolari and Acosta, 2007). Free D-Asp is found in a wide variety of mammalian tissues and cells, particularly in the central nervous and endocrine systems, and several lines of evidence have suggested that D-Asp plays an important role in regulating developmental processes, hormone secretion, and steroidogenesis (for review see D'Aniello, 2007; Homma, 2007).

In mammalian tissues, two types of degradative enzymes that are stereospecific for D-amino acids have been identified, D-amino acid oxidase (DAAO, also abbreviated to DAO, EC 1.4.3.3) and D-Asp oxidase (DASPO, also abbreviated to DDO, EC 1.4.3.1). DAAO and DASPO are flavin adenine dinucleotide (FAD)-containing flavoproteins that catalyze the oxidative deamination of D-amino acids with oxygen to generate the corresponding 2-oxo acids, along with hydrogen peroxide and ammonium ions. The two enzymes are similar in molecular mass, primary structure, and catalytic specificity, but differ markedly in their substrate specificity. DAAO displays broad substrate specificity and acts on several neutral and basic D-amino acids, while DASPO is highly specific for acidic D-amino acids, such as D-Asp, NMDA, and D-Glu, none of which

are substrates of DAAO. Although DAAO and DASPO have been found in various organisms, their physiological roles in vivo have yet to be fully clarified. Konno and Yasumura (1983) isolated a mouse mutant that lacks DAAO activity (ddY/DAO$^-$) that has higher D-Ser levels in its central nervous system and serum than wild-type ddY/DAO$^+$ mice (Hashimoto et al., 1993). The location of DAAO in rat brain was found to correlate inversely with the presence of D-Ser (Schell et al., 1995). Similarly, the location of DASPO in rat tissue correlates inversely with the presence of D-Asp (Schell et al., 1997). Two groups recently established DASPO-deficient mice independently, and it was shown that these mice have significantly elevated levels of D-Asp in several tissues (Errico et al., 2006; Huang et al., 2006). Thus, evidence to date suggests that mammalian DAAO and DASPO regulate endogenous D-Ser and D-Asp levels, respectively, by metabolizing these D-amino acids, in addition to mediating the elimination of accumulated exogenous D-amino acids in various organs.

With regard to the structural properties of DAAO, extensive mutagenesis of recombinant DAAO has identified important structural amino acid residues of DAAO (Sacchi et al., 2002; Setoyama et al., 2002, 2006; Boselli et al., 2004; Caldinelli et al., 2006; for reviews, see Pilone, 2000 and references cited therein). The 3-dimensional (3D) structures of porcine, *Rhodotorula gracilis* and human DAAO have also been determined by X-ray crystallography (Mattevi et al., 1996; Mizutani et al., 1996; Miura et al., 1997; Umhau et al., 2000; Kawazoe et al., 2006). These studies have identified amino acid residues in the active site of DAAO that play a significant role in enzymatic activity (see Fig. 1A and B). In contrast, DASPO is less well understood, as there have been few studies that have analyzed the structural properties of DASPO, and the 3D crystal structure of DASPO has yet to be reported.

We recently cloned a cDNA that encodes DASPO from mouse kidney (GenBank accession number: AB274968) and proposed a structural model of murine DASPO (mDASPO) based on the deduced amino acid sequence (Katane et al., 2007a). In our proposed structure, the side chains of Arg-216, Tyr-223, Arg-237, Arg-278, and Ser-308 are oriented toward the predicted binding pocket of the active site (see Fig. 1C), which implicates these residues in mDASPO catalysis. Arg-216, Tyr-223, Arg-237, Arg-278, and Ser-308 of mDASPO are conserved in all of the mammalian DASPOs that have been cloned to date. Tyr-223 and Arg-278 are also conserved in all mammalian and yeast DAAOs, whereas Arg-216, Arg-237, and Ser-308 are not well conserved in DAAOs. Previously, we

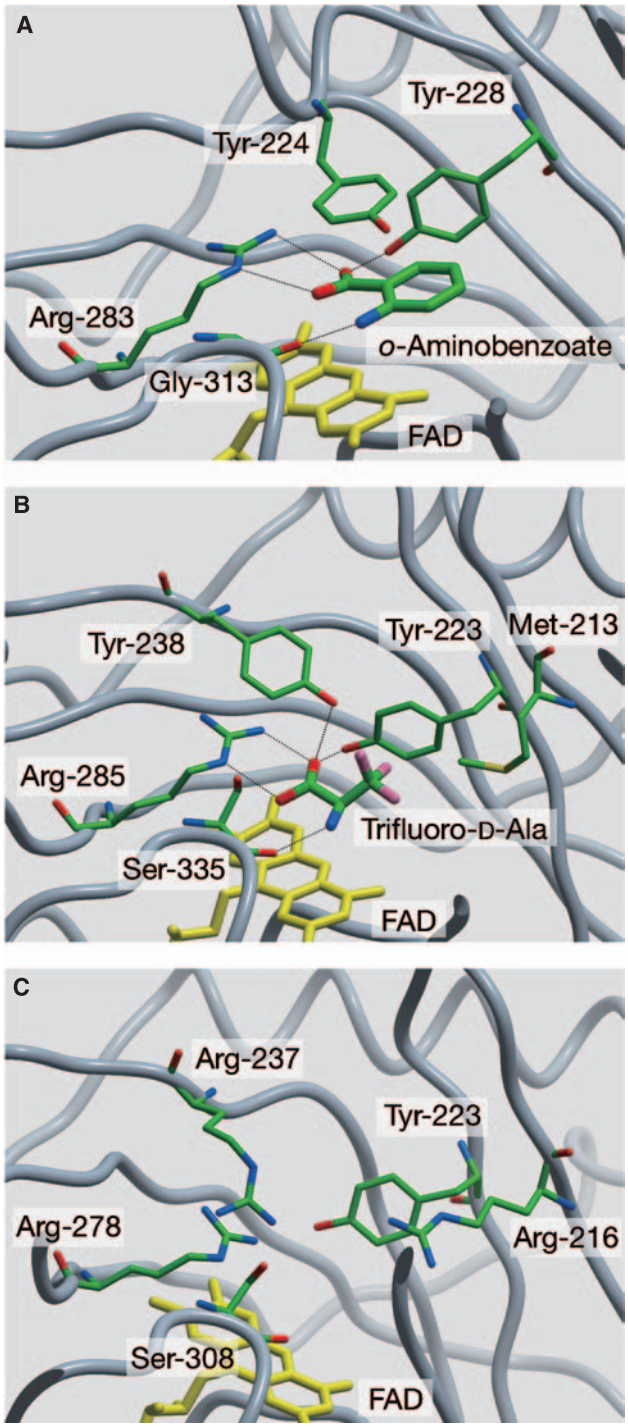

Fig. 1. Mapping of key catalytic residues in the active site of mDASPO using a predicted 3D structure. Experimentally determined structures of porcine DAAO complexed with *o*-aminobenzoate (Protein Data Bank ID: 1AN9) (Miura et al., 1997) and *R. gracilis* DAAO complexed with trifluoro-D-Ala (Protein Data Bank ID: 1C0L) (Umhau et al., 2000) are shown in **A** and **B**, respectively. A proposed structural model of mDASPO is shown in **C** (for details of the modeling method, see Katane et al., 2007a). Bound ligands and side chains of amino acid residues that have been demonstrated or are believed to be catalytically important are colored according to the atom type: carbon, green; nitrogen, blue; oxygen, red; fluorine, magenta; sulfur, khaki. FAD molecules are colored yellow while dotted lines denote hydrogen bonds and electrostatic interactions

demonstrated that Arg-216 and Arg-237 of mDASPO are catalytically important residues, using a mutagenesis approach (Katane et al., 2007a). In the current study, using a similar approach, we examined whether Ser-308, particularly its side chain hydroxyl group, also contributed to the enzymatic properties of mammalian DASPO. We prepared several recombinant mDASPO mutants in which Ser-308 was substituted with other amino acid residues and examined their enzymatic and kinetic properties. We found that Gly- and Ala-substitution mutants, which lacked a hydroxyl group at position 308, had a significantly higher catalytic efficiency and affinity for FAD than the wild-type enzyme, while the Tyr-substitution mutant, which contained a hydroxyl group at position 308, had a lower catalytic efficiency and binding capacity. These results suggest that the side chain hydroxyl group of Ser-308 down-regulates the enzymatic activity, substrate binding and FAD binding of mDASPO, and provide novel and useful insight into the structure-function relationship of mammalian DASPO.

Materials and methods

Chemicals

D- and L-amino acids, bovine serum albumin, and *Aspergillus niger* catalase were purchased from Sigma-Aldrich (St Louis, MO, USA). FAD, isopropyl-β-D-thiogalactopyranoside, and imidazole were purchased from Wako Pure Chemical Industries (Osaka, Japan). Other chemicals were of the highest grade available and purchased from commercial sources.

Construction of recombinant protein expression plasmids

The expression plasmid for N-terminal His-tagged mDASPO (His-mDASPO) (pRSET-His-mDASPO) has been described previously (Katane et al., 2007a). To construct the expression plasmid for mDASPO fused N-terminally with glutathione *S*-transferase (GST), His, and S (GHS) (GHS-mDASPO), a 1.1-kb *Nco*I-*Hin*dIII fragment from pRSET-His-mDASPO containing the entire mDASPO-coding sequence was subcloned into pET-41a(+) (Novagen, Madison, WI, USA) (pET-GHS-mDASPO).

Ser-308-to-Gly (S308G), Ser-308-to-Ala (S308A), and Ser-308-to-Tyr (S308Y) substitutions were introduced into pRSET-His-mDASPO by site-directed mutagenesis using the QuikChange II Site-Directed Mutagenesis Kit (Stratagene, La Jolla, CA, USA) to generate expression plasmids for N-terminal His-tagged S308G, S308A, and S308Y mutants (pRSET-His-mDASPO-S308G, pRSET-His-mDASPO-S308A, and pRSET-His-mDASPO-S308Y, respectively). The following mutagenic oligonucleotides were used (mutated codons are underlined):

for S308G, 5′-CGGCCACGGGGGTGGGGGCATCT-3′ and 5′-AGATG CCCCCACCCCCGTGGCCG-3′;
for S308A, 5′-CGGCCACGGGGCTGGGGGCATCT-3′ and 5′-AGATG CCCCCAGCCCCGTGGCCG-3′;
for S308Y, 5′-CGGCCACGGGTATGGGGGCATCT-3′ and 5′-AGATG CCCCCATACCCGTGGCCG-3′.

All mutations were confirmed by sequencing. A 1.1-kb *Nco*I-*Hin*dIII fragment of pRSET-His-mDASPO-S308G, pRSET-His-mDASPO-S308A, or pRSET-His-mDASPO-S308Y was subcloned into pET-41a(+) to generate expression plasmids for N-terminal GHS-tagged S308G, S308A, and S308Y mutants (pET-GHS-mDASPO-S308G, pET-GHS-mDASPO-S308A, and pET-GHS-mDASPO-S308Y, respectively).

Expression and purification of recombinant proteins

Escherichia coli strain BL21(DE3)pLysS was transformed with expression plasmids and grown at 37 °C with shaking in LB medium containing ampicillin (100 μg/ml). When the cultures reached an A_{620} of 0.5, the temperature was decreased to 30 °C and the cells were grown for an additional 30 min. The culture temperature was further decreased to 26 °C and the cells were grown for an additional 30 min, then isopropyl-β-D-thiogalactopyranoside was added to a final concentration of 0.1 mM, and the cells were grown at 26 °C for 16 h. The cells were subjected to centrifugation at 10,000 × *g* for 10 min at 4 °C, and crude extract and insoluble fraction were prepared as described previously (Katane et al., 2007b). In some cases, Lysonase Bioprocessing Reagent (Novagen) was used to increase protein extraction efficiency and overall protein yield (10 μl of the reagent per g of wet cell paste).

GHS- or His-tagged recombinant proteins were purified by affinity chromatography using a chelating column. Crude extracts prepared as described above were applied to a His GraviTrap column (GE Healthcare Bio-Sciences, Piscataway, NJ, USA) equilibrated with 20 mM sodium phosphate buffer (pH 7.4) that contained 0.5 M NaCl and 10 mM imidazole. The column was washed with the same buffer and the bound proteins were eluted in a step-wise gradient of 50–500 mM imidazole. The fraction (2 ml) that eluted at 400 mM imidazole and contained recombinant protein was mixed with 50 μl of 2 mM FAD and dialyzed for 3 h twice against 1 l of 10 mM sodium pyrophosphate buffer (pH 8.3) containing 2 mM EDTA, 5 mM 2-mercaptoethanol, and 10% glycerol. The dialyzed fraction containing purified enzyme was recovered and used immediately for enzyme assays or stored frozen at −80 °C until use. From 2 and 3 g of wet cell paste, 0.8 and 0.2 mg of purified GHS- and His-tagged recombinant proteins, respectively, were obtained. To prepare apoenzyme, FAD was omitted from all the procedures described above. The apoenzyme preparation exhibited no residual activity in the absence of FAD.

Detection of recombinant proteins

The concentration of protein in crude extracts, insoluble fractions, and purified preparations was determined by the method of Bradford (1976) (Bio-Rad Protein Assay, Bio-Rad Laboratories, Hercules, CA, USA) using bovine serum albumin as a standard. Crude extracts (20 μg), insoluble fractions (20 μg), and purified enzyme preparations (0.5 μg) were subjected to SDS-PAGE (10% gel) and Western blot using a rabbit anti-His-tag antibody (His-probe, Santa Cruz Biotechnology, Santa Cruz, CA, USA) (1:1,000 dilution) or a mouse anti-GST antibody (Anti-GST Mouse IgG2a-κ, Nacalai Tesque, Kyoto, Japan) (1:1,000 dilution) as the primary antibody, and horseradish peroxidase-conjugated anti-rabbit IgG (Jackson ImmunoResearch Laboratories, West Grove, PA, USA) (1:5,000 dilution) or horseradish peroxidase-conjugated anti-mouse IgG (Jackson ImmunoResearch Laboratories) (1:5,000 dilution) as the secondary antibody. To determine protein purity, purified enzyme preparations (0.5 or 1.0 μg) were separated on a 10 or 12% SDS-polyacrylamide gel and visualized using Coomassie Brilliant Blue R-250. The purity of all of the mutants examined in this study was equivalent to that of the wild-type enzyme.

Assays of enzymatic activity

Oxidase activities were determined using a colorimetric assay for the production of 2-oxo acid, as previously described in detail (Katane et al., 2007b). Briefly, purified enzyme (0.1–5.0 μg) was mixed in a reaction mixture consisting of 40 mM sodium pyrophosphate buffer (pH 8.3), 23 units of *A. niger* catalase, 50 μM FAD, and 20 mM amino acid in a final volume of 150 μl, and incubated at 37 °C. Preliminary experiments showed that the production of 2-oxo acids was linear for a period of 20 min under these assay conditions for all of the recombinant purified enzymes and

amino acids examined in this study. Thus, the reaction time was set at 15 min. After 15 min, 10 µl of 100% (w/v) trichloroacetic acid was added to stop the reaction. The 2-oxo acid product was then reacted with 2,4-dinitrophenylhydrazine and quantified by measuring the absorbance at 445 nm. Reaction mixtures that lacked amino acids served as the negative controls (blanks). One unit of enzyme activity was defined as the production of 1 µmol of 2-oxo acid per min. To determine the V_{max} (maximal velocity) and K_m (Michaelis constant) values for D-Asp and NMDA, different final concentrations (0, 1, 2, 5, 10, 20, and 40 mM) of amino acids were used as substrates. To determine the K_d (dissociation constant) value for FAD binding ($K_{d,\ FAD}$), 0.7–4.2 µg of purified apoenzyme were mixed in a reaction mixture consisting of 50 mM sodium pyrophosphate buffer (pH 8.3), 23 units of *A. niger* catalase, and varying final concentrations (0, 0.125, 0.25, 0.625, 1.25, 2.5, 6.25, and 12.5 µM) of FAD in a final volume of 120 µl. After a 20 min preincubation period at 4 °C, 30 µl of 100 mM D-Asp were added, followed by incubation at 37 °C for 15 min. Enzymatic activity was then determined as described above. In some cases, the enzymatic reaction was performed with air-saturated 40 mM sodium pyrophosphate buffer (pH 8.3) ($[O_2] = 0.24–0.26$ mM).

Results and discussion

Purification of the recombinant mutant proteins

We first constructed an expression plasmid for GHS-mDASPO, in which the GST-tag as well as a His- and S-tag were fused to the N-terminus of mDASPO. GHS-mDASPO is a 620 amino acid protein with a calculated molecular mass of 69,256 Da. *E. coli* strain BL21(DE3)-pLysS cells were transformed with the GHS-mDASPO expression plasmid, and the crude extract and insoluble fraction were subjected to Western blot analysis. Recombinant GHS-mDASPO was detected in the crude extract (data not shown) at an apparent molecular mass that corresponded to the theoretical mass deduced from its amino acid sequence. The insoluble fraction also exhibited an intensely positive band with the same mobility (data not shown). Thus, recombinant GHS-mDASPO, similar to recombinant His-mDASPO (Katane et al., 2007a), was expressed in both a soluble and insoluble form.

We purified recombinant GHS-mDASPO as described in Materials and methods. The purified preparation consisted primarily of recombinant full-length GHS-mDASPO, although a protein band with a lower molecular mass (approximately 27 kDa) was also observed when examined by SDS-PAGE (data not shown). This low molecular weight protein likely represented a degradation product of GHS-mDASPO that retained the GHS-tag, rather than a contaminating endogenous *E. coli* protein, since the 27 kDa protein reacted with antibodies against His and GST (data not shown).

To examine the role of Ser-308 in mDASPO catalysis, we constructed three mutant GHS-mDASPO derivatives in which the Ser-308 codon was mutated to a Gly, Ala, or Tyr codon. While Gly lacks a side chain hydroxyl group, when the amino acid sequences of porcine DAAO and mDASPO are aligned, Ser-308 of mDASPO corresponds to Gly-313 of porcine DAAO, and Gly-313 appears to be conserved in all mammalian and yeast DAAOs, with the exception of *R. gracilis* (data not shown). The alignment of Ser-308 of mDASPO and Gly-313 of DAAO was also observed when we compared the 3D structure of porcine DAAO and the structural model of mDASPO (Fig. 1A and C). We constructed the S308G mutant to determine whether Gly could substitute for Ser at position 308 of mDASPO. As a control for steric hindrance, we generated S308A, which inserted a non-polar residue that also lacked a hydroxyl group at position 308. Finally, S308Y served as a non-conservative substitution mutant of Ser-308, but nevertheless retained the side chain hydroxyl group at this position. The mutant proteins were purified as described in Materials and methods.

Characterization of the enzymatic and kinetic properties of the purified proteins

We examined the enzymatic activity of the purified recombinant proteins against several different amino acids. Wild-type GHS-mDASPO exhibited similar levels of activity towards D-Asp and NMDA, and relatively low activity towards D-Glu (Table 1). Activity was very low or undetectable when the enantiomers L-Asp, *N*-methyl-L-Asp, and L-Glu, and all neutral (D-Asn, D-Ala and D-Phe) and basic (D-Arg and D-Lys) D-amino acids were used in the reaction mixture. These results were consistent with our previous report of the substrate specificity of recombinant mDASPO and His-mDASPO (Katane et al., 2007a), and confirmed that mDASPO is highly specific for D-Asp and NMDA. Similar to wild-type GHS-mDASPO, all of the mutants exhibited activity towards acidic D-amino acids. The activities of the S308G

Table 1. Oxidase activities of purified recombinant GHS-mDASPO and its mutant derivatives against acidic D-amino acids

Substrates	Specific activity (U/mg protein)			
	Wild-type	S308G mutant	S308A mutant	S308Y mutant
D-Asp	4.31 ± 0.14	9.24 ± 0.61	5.55 ± 0.55	2.37 ± 0.09
NMDA	4.32 ± 0.17	13.1 ± 0.63	5.92 ± 0.03	2.54 ± 0.35
D-Glu	0.10 ± 0.01	0.55 ± 0.04	0.24 ± 0.04	0.11 ± 0.01

Enzymatic activities were assayed at 37 °C in 40 mM sodium pyrophosphate buffer (pH 8.3). Data represent the means ± standard deviation of three independent assays. *1 U* 1 µmol substrate oxidized per min

Table 2. Apparent steady-state kinetic parameters of purified recombinant GHS-mDASPO and its mutant derivatives

Enzymes	V_{max} (U/mg protein)		K_m (mM)		$K_{d,\ FAD}$ (μM)
	D-Asp	NMDA	D-Asp	NMDA	
Wild-type	5.34 ± 0.13	5.44 ± 0.13	4.87 ± 0.37	6.59 ± 0.47	1.06 ± 0.06
S308G mutant	9.61 ± 0.33	13.9 ± 0.73	1.20 ± 0.12	1.95 ± 0.36	0.50 ± 0.10
S308A mutant	5.86 ± 0.27	7.07 ± 0.32	1.78 ± 0.30	4.23 ± 0.39	0.57 ± 0.04
S308Y mutant	3.25 ± 0.16	3.59 ± 0.56	7.63 ± 0.26	7.81 ± 0.38	5.72 ± 0.90

Steady-state reactions were performed at 37 °C in air-saturated 40 mM sodium pyrophosphate buffer (pH 8.3) ($[O_2] = 0.24–0.26$ mM). Data represent the means ± standard deviation of three independent assays. *1 U* 1 μmol substrate oxidized per min

and S308A mutants, however, were reproducibly higher than that of the wild-type enzyme. In contrast, the activity of the S308Y mutant towards D-Asp and NMDA was lower than the wild-type enzyme, while its activity towards D-Glu was similar to wild-type. All of the mutants had very low or undetectable activity with substrates other than acidic D-amino acids. Thus, the S308G, S308A, and S308Y mutants retained the ability of the wild-type enzyme to catalyze the deamination of acidic D-amino acids, although the relative activity levels of each differed significantly. These results indicated that while Ser-308 of mDASPO does not function as a catalytic site residue that is directly involved in deprotonation of substrates, it appears to play a critical role in the activity of the enzyme.

We next generated plots of $[S]/v$ versus $[S]$ (data not shown) to determine the apparent kinetic parameters of deamination of D-Asp and NMDA by the purified recombinant proteins (Table 2). It has been reported that bovine, porcine and octopus DASPO do not follow classic Michaelis-Menten kinetics, as they exhibit substrate activation or inhibition (Negri et al., 1988; Tedeschi et al., 1994; Yamamoto et al., 2007). We determined the kinetic parameters of mDASPO in air-saturated buffer ($[O_2] = 0.24–0.26$ mM) at substrate concentrations in the range of 1.0–40 mM, in which Michaelis-Menten behavior was observed and a linear relationship of $[S]/v$ versus $[S]$ was obtained. The V_{max} values of the S308G and S308A mutants towards D-Asp and NMDA were markedly higher than those of the wild-type enzyme, and the K_m values against D-Asp and NMDA were reproducibly lower than wild-type. Therefore, the catalytic efficiency (expressed as V_{max}/K_m) of the S308G mutant in the presence of D-Asp and NMDA was approximately 7.3 and 8.8 times higher, respectively, than the wild-type enzyme (Fig. 2A). Similarly, the S308A mutant was approximately 3.1 and 2.0 times more efficient in the presence of D-Asp and NMDA, respectively, compared to the wild-type enzyme. In contrast, the V_{max} values of the S308Y mutant towards D-Asp and NMDA were lower than that of the wild-type enzyme, and the K_m values were higher (Table 2). This

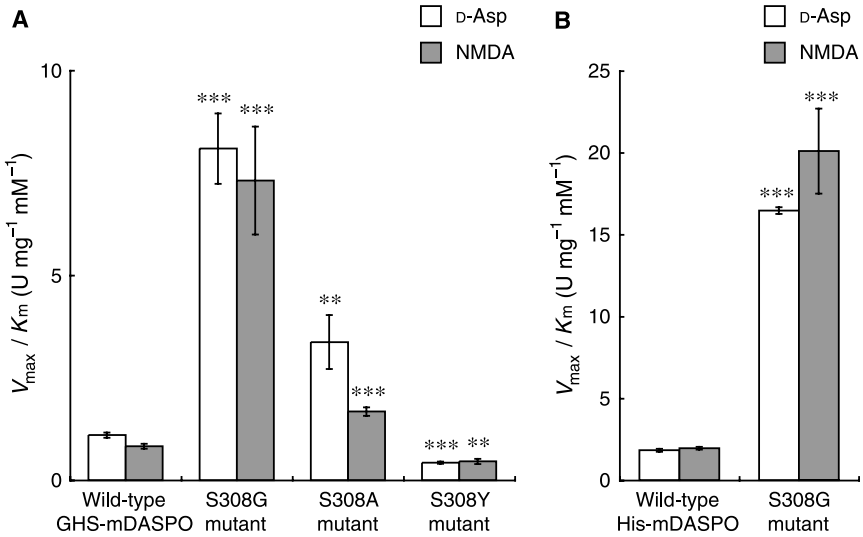

Fig. 2. Comparison of the catalytic efficiency of the purified recombinant proteins towards D-Asp and NMDA. Enzymatic activities were assayed using the indicated purified enzymes. V_{max}/K_m values for D-Asp (*white bars*) and NMDA (*grey bars*) were calculated from the V_{max} and K_m values listed in Tables 2 and 3 in **A** and **B**, respectively. Data represent the means ± standard deviation of three independent assays. $^{**}p < 0.01$ (Student's *t*-test) versus wild-type GHS-mDASPO. $^{***}p < 0.001$ (Student's *t*-test) versus wild-type GHS-mDASPO or His-mDASPO

resulted in a catalytic efficiency of the S308Y mutant in the presence of D-Asp and NMDA that was approximately 2.6 and 1.8 times lower than that of the wild-type enzyme, respectively (Fig. 2A). These results indicated that the side chain hydroxyl group of Ser-308 of mDASPO down-regulates the enzymatic activity and substrate binding of mDASPO.

Ser-308 is thought to lie proximal to the flavin ring of FAD (Fig. 1C). To determine whether substitution of Ser-308 affected its affinity for FAD, we obtained plots of [FAD]/v versus [FAD] (data not shown) and determined the $K_{d,\ FAD}$ values of purified apoenzymes. The $K_{d,\ FAD}$ value of the wild-type enzyme was $[1.06 \pm 0.06] \times 10^{-6}$ M (means $\pm$ standard deviation of three independent assays). This value was relatively higher than the reported $K_{d,\ FAD}$ values of bovine and *Cryptococcus humicola* DASPOs (5.0×10^{-8} and 8.2×10^{-12} M, respectively) (Negri et al., 1987; Iwazaki et al., 2000). In addition, the reported $K_{d,\ FAD}$ values of mammalian and yeast DAAOs are on the order of 10^{-6}–10^{-8} M (Massey and Ganther, 1965; Casalin et al., 1991; Molla et al., 2006). Thus, the FAD-binding affinity of mDASPO appeared to be rather weak. The $K_{d,\ FAD}$ values of the S308G and S308A mutants were slightly but reproducibly lower than that of the wild-type enzyme (Table 2). Thus, the introduction of a S308G or S308A mutation into GHS-mDASPO increased its catalytic efficiency in the presence of D-Asp and NMDA, and increased its ability to bind to FAD. The $K_{d,\ FAD}$ value of the S308Y mutant was approximately 5.4 times higher than that of the wild-type enzyme. These results suggested that the conformation of the region involving residue 308 in the S308G and S308A mutants is more suitable for catalysis and FAD binding than the wild-type enzyme or the S308Y mutant.

Hyperactivity of the His-tagged recombinant S308G substitution mutant

To improve the recovery of recombinant mDASPO and confirm the hyperactivity of the S308G mutant, we examined the expression, purity, and activity of recombinant His-mDASPO, since this protein can be purified to homogeneity. Although the purification yield was lower than that of GHS-mDASPO, SDS-PAGE analysis revealed that recombinant His-mDASPO was purified to near-homogeneity (data not shown). Subsequently, we constructed a mutant derivative of His-mDASPO in which the codon for Ser-308 was mutated to a Gly codon, and the S308G mutant was purified to near-homogeneity, similar to the wild-type enzyme.

Table 3. Apparent steady-state kinetic parameters of purified recombinant His-mDASPO and the S308G mutant

Enzymes	V_{max} (U/mg protein)		K_m (mM)	
	D-Asp	NMDA	D-Asp	NMDA
Wild-type	13.3 ± 0.94	15.6 ± 1.42	7.30 ± 0.38	8.02 ± 0.68
S308G mutant	39.0 ± 2.39	53.0 ± 2.60	2.37 ± 0.12	2.67 ± 0.45

Steady-state reactions were performed at 37 °C in air-saturated 40 mM sodium pyrophosphate buffer (pH 8.3) ($[O_2] = 0.24$–0.26 mM). Data represent the means $\pm$ standard deviation of three independent assays. *1 U* 1 μmol substrate oxidized per min

We then examined the enzymatic activity of the purified recombinant proteins towards acidic D-amino acids. Based on the results of three independent assays, the specific activity of wild-type His-mDASPO towards D-Asp, NMDA and D-Glu was 9.91 ± 0.47, 11.4 ± 0.64 and 0.26 ± 0.07 U/mg protein, respectively. The specific activity of the S308G mutant towards D-Asp, NMDA and D-Glu was 35.3 ± 1.45, 47.2 ± 1.89 and 2.06 ± 0.13 U/mg protein, respectively, which was approximately 3.6–7.8 times higher than that of the wild-type enzyme. The plots of [S]/v versus [S] for the deamination of D-Asp and NMDA revealed that the V_{max} value of the S308G mutant in the presence of D-Asp and NMDA was markedly higher than the wild-type enzyme (Table 3). In addition, the K_m values of the S308G mutant were reproducibly lower than wild-type His-mDASPO. Thus, the catalytic efficiency of the S308G mutant in the presence of D-Asp and NMDA was approximately 9.0 and 10 times higher than that of the wild-type enzyme, respectively (Fig. 2B). These observations confirmed that the introduction of a S308G mutation into mDASPO significantly increases its catalytic efficiency. The differences in the V_{max} and K_m values of the wild-type and S308G mutant enzymes between Tables 2 and 3 may reflect a distinctive steric hindrance caused by their N-terminal tag, since the calculated molecular masses of the GHS- and His-tag are considerably different.

In conclusion, we demonstrated that Ser-308 is a critical residue in catalysis by mDASPO, and that the side chain hydroxyl group of this residue unexpectedly down-regulates enzymatic activity, substrate binding and FAD binding of mDASPO. Previously, it was shown that mutation of the spatially equivalent residue in *R. gracilis* DAAO (Ser-335) lowered catalytic activity compared to wild-type DAAO (Boselli et al., 2004). The authors proposed that the side chain hydroxyl group of Ser-335 of *R. gracilis* DAAO functions in transferring a proton from

the substrate to the solvent. In contrast to the *R. gracilis* DAAO mutant, the S308G and S308A mutants of mDASPO are catalytically more efficient towards D-Asp and NMDA than the wild-type enzyme (Fig. 2). Moreover, even though the S308Y mutant had a side chain hydroxyl group at position 308, its catalytic efficiency towards D-Asp and NMDA was lower than that of the wild-type enzyme. Thus, it is possible that the role of Ser-308 in mDASPO catalysis differs from that of Ser-335 in *R. gracilis* DAAO catalysis. The side chain hydroxyl group of Ser-308 apparently down-regulates the catalytic efficiency of mDASPO, although the mechanism of regulation of enzymatic activity by the side chain is unclear, as is the mechanism by which S308G and S308A substitutions result in mDASPO hyperactivity. Additional studies to elucidate the crystal structures of wild-type and mutant mDASPO are certainly needed.

Acknowledgements

The authors would like to thank Misses Mariko Tomita, Masumi Iizuka, Noriko Nakamura, and Sanae Nagai for technical assistance. This work was supported by a Grant-in-Aid for Scientific Research (18790062 to M.K.) from the Japan Society for the Promotion of Science. This work was also supported in part by the Kitasato University Research Grant for Young Researchers (M.K.).

References

Abe H, Yoshikawa N, Sarower MG, Okada S (2005) Physiological function and metabolism of free D-alanine in aquatic animals. Biol Pharm Bull 28: 1571–1577

Boselli A, Piubelli L, Molla G, Sacchi S, Pilone MS, Ghisla S, Pollegioni L (2004) On the mechanism of *Rhodotorula gracilis* D-amino acid oxidase: role of the active site serine 335. Biochim Biophys Acta 1702: 19–32

Bradford MM (1976) A rapid and sensitive method for the quantitation of microgram quantities of protein utilizing the principle of protein-dye binding. Anal Biochem 72: 248–254

Caldinelli L, Molla G, Pilone MS, Pollegioni L (2006) Tryptophan 243 affects interprotein contacts, cofactor binding and stability in D-amino acid oxidase from *Rhodotorula gracilis*. FEBS J 273: 504–512

Casalin P, Pollegioni L, Curti B, Pilone MS (1991) A study on apoenzyme from *Rhodotorula gracilis* D-amino acid oxidase. Eur J Biochem 197: 513–517

D'Aniello A (2007) D-Aspartic acid: an endogenous amino acid with an important neuroendocrine role. Brain Res Rev 53: 215–234

Errico F, Pirro MT, Affuso A, Spinelli P, De Felice M, D'Aniello A, Di Lauro R (2006) A physiological mechanism to regulate D-aspartic acid and NMDA levels in mammals revealed by D-aspartate oxidase deficient mice. Gene 374: 50–57

Fujii N (2005) D-Amino acid in elderly tissues. Biol Pharm Bull 28: 1585–1589

Hamase K, Konno R, Morikawa A, Zaitsu K (2005) Sensitive determination of D-amino acids in mammals and the effect of D-amino-acid oxidase activity on their amounts. Biol Pharm Bull 28: 1578–1584

Hashimoto A, Nishikawa T, Konno R, Niwa A, Yasumura Y, Oka T, Takahashi K (1993) Free D-serine, D-aspartate and D-alanine in central nervous system and serum in mutant mice lacking D-amino acid oxidase. Neurosci Lett 152: 33–36

Homma H (2007) Biochemistry of D-aspartate in mammalian cells. Amino Acids 32: 3–11

Huang AS, Beigneux A, Weil ZM, Kim PM, Molliver ME, Blackshaw S, Nelson RJ, Young SG, Snyder SH (2006) D-Aspartate regulates melanocortin formation and function: behavioral alterations in D-aspartate oxidase-deficient mice. J Neurosci 26: 2814–2819

Iwazaki I, Yamashita S, Arimoto K, Takahashi M, Kera Y, Yamada R (2000) Apoenzyme from *Cryptococcus humicolus* UJ1 D-aspartate oxidase. J Mol Catal B 10: 183–189

Katane M, Furuchi T, Sekine M, Homma H (2007a) Molecular cloning of a cDNA encoding mouse D-aspartate oxidase and functional characterization of its recombinant proteins by site-directed mutagenesis. Amino Acids 32: 69–78

Katane M, Seida Y, Sekine M, Furuchi T, Homma H (2007b) *Caenorhabditis elegans* has two genes encoding functional D-aspartate oxidases. FEBS J 274: 137–149

Kawazoe T, Tsuge H, Pilone MS, Fukui K (2006) Crystal structure of human D-amino acid oxidase: context-dependent variability of the backbone conformation of the VAAGL hydrophobic stretch located at the *si*-face of the flavin ring. Protein Sci 15: 2708–2717

Konno R, Yasumura Y (1983) Mouse mutant deficient in D-amino acid oxidase activity. Genetics 103: 277–285

Massey V, Ganther H (1965) On the interpretation of the absorption spectra of flavoproteins with special reference to D-amino acid oxidase. Biochemistry 4: 1161–1173

Mattevi A, Vanoni MA, Todone F, Rizzi M, Teplyakov A, Coda A, Bolognesi M, Curti B (1996) Crystal structure of D-amino acid oxidase: a case of active site mirror-image convergent evolution with flavocytochrome b_2. Proc Natl Acad Sci USA 93: 7496–7501

Miura R, Setoyama C, Nishina Y, Shiga K, Mizutani H, Miyahara I, Hirotsu K (1997) Structural and mechanistic studies on D-amino acid oxidase-substrate complex: implications of the crystal structure of enzyme-substrate analog complex. J Biochem (Tokyo) 122: 825–833

Mizutani H, Miyahara I, Hirotsu K, Nishina Y, Shiga K, Setoyama C, Miura R (1996) Three-dimensional structure of porcine kidney D-amino acid oxidase at 3.0 Å resolution. J Biochem (Tokyo) 120: 14–17

Mizutani H, Miyahara I, Hirotsu K, Nishina Y, Shiga K, Setoyama C, Miura R (2000) Three-dimensional structure of the purple intermediate of porcine kidney D-amino acid oxidase. Optimization of the oxidative half-reaction through alignment of the product with reduced flavin. J Biochem (Tokyo) 128: 73–81

Molla G, Sacchi S, Bernasconi M, Pilone MS, Fukui K, Pollegioni L (2006) Characterization of human D-amino acid oxidase. FEBS Lett 580: 2358–2364

Negri A, Massey V, Williams CH Jr (1987) D-Aspartate oxidase from beef kidney. Purification and properties. J Biol Chem 262: 10026–10034

Negri A, Massey V, Williams CH Jr, Schopfer LM (1988) The kinetic mechanism of beef kidney D-aspartate oxidase. J Biol Chem 263: 13557–13563

Pilone MS (2000) D-Amino acid oxidase: new findings. Cell Mol Life Sci 57: 1732–1747

Sacchi S, Lorenzi S, Molla G, Pilone MS, Rossetti C, Pollegioni L (2002) Engineering the substrate specificity of D-amino-acid oxidase. J Biol Chem 277: 27510–27516

Schell MJ (2004) The *N*-methyl D-aspartate receptor glycine site and D-serine metabolism: an evolutionary perspective. Phil Trans R Soc London Ser B 359: 943–964

Schell MJ, Cooper OB, Snyder SH (1997) D-Aspartate localizations imply neuronal and neuroendocrine roles. Proc Natl Acad Sci USA 94: 2013–2018

Schell MJ, Molliver ME, Snyder SH (1995) D-Serine, an endogenous synaptic modulator: localization to astrocytes and glutamate-stimulated release. Proc Natl Acad Sci USA 92: 3948–3952

Scolari MJ, Acosta GB (2007) D-Serine: a new word in the glutamatergic neuro-glial language. Amino Acids 33: 563–574

Setoyama C, Nishina Y, Mizutani H, Miyahara I, Hirotsu K, Kamiya N, Shiga K, Miura R (2006) Engineering the substrate specificity of porcine kidney D-amino acid oxidase by mutagenesis of the ''active-site lid''. J Biochem (Tokyo) 139: 873–879

Setoyama C, Nishina Y, Tamaoki H, Mizutani H, Miyahara I, Hirotsu K, Shiga K, Miura R (2002) Effects of hydrogen bonds in association with flavin and substrate in flavoenzyme D-amino acid oxidase. The catalytic and structural roles of Gly313 and Thr317. J Biochem (Tokyo) 131: 59–69

Tedeschi G, Negri A, Ceciliani F, Ronchi S, Vetere A, D'Aniello G, D'Aniello A (1994) Properties of the flavoenzyme D-aspartate oxidase from *Octopus vulgaris*. Biochim Biophys Acta 1207: 217–222

Umhau S, Pollegioni L, Molla G, Diederichs K, Welte W, Pilone MS, Ghisla S (2000) The X-ray structure of D-amino acid oxidase at very high resolution identifies the chemical mechanism of flavin-dependent substrate dehydrogenation. Proc Natl Acad Sci USA 97: 12463–12468

Yamamoto A, Tanaka H, Ishida T, Horiike K (2007) Functional and structural characterization of D-aspartate oxidase from porcine kidney: non-Michaelis kinetics due to substrate activation. J Biochem (Tokyo) 141: 363–376

Authors' address: Hiroshi Homma, Laboratory of Biomolecular Science, School of Pharmaceutical Sciences, Kitasato University, 5-9-1 Shirokane, Minato-ku, Tokyo 108-8641, Japan,
Fax: +81-3-5791-6381, E-mail: hommah@pharm.kitasato-u.ac.jp